Energy Transfer to the Low-Energy Triplet States of 1,3-Dicarbonylazomethine Dyes: The Role of Unique Geometries and Nonadiabatic Behavior

Faraj Abu-Hasanayn*,† and William G. Herkstroeter*,‡

Imaging Research and Advanced Development, Eastman Kodak Company, Rochester, New York 14650, and Department of Chemistry, University of Rochester, Rochester, New York 14627-0216

Received: August 2, 2000; In Final Form: November 28, 2000

The observed kinetics of energy transfer to PhCO−(C═NAr)−CONHPh (**1**), PhCO−(C═NAr)−COPh (**2**), and PhCONH−(C═NAr)−CONHPh (**3**) (Ar = p-$NMe_2C_6H_4$) is consistent with formation of two triplet states for each dye: T_1 and T_2. A Balzani analysis of the data observed for **1** affords triplet energies of 23.4 ± 1.6 and 38.5 ± 1.7 kcal/mol for T_1 and T_2, respectively, and requires that T_1 be formed in reactions having substantial nonadiabatic character. A similar result is found for **2**. For **3**, T_1 and T_2 are estimated at 25.0 and 38.5 kcal/mol, respectively, but formation of **3**-T_1 is found to be largely adiabatic. To rationalize these observations, the dyes have been studied by DFT methods (B3LYP/6-31G*). In the ground state (**1**-S_0) **1** is computed to have a geometry in which the azomethine double bond is coplanar with the anilide fragment but is perpendicular to the carbonyl of the ketone. Similarly, **2**-S_0 is calculated to have a twisted 1,3-dicarbonyl arrangement. **3**-S_0, on the other hand, exhibits an intramolecular H-bond between the proton of one anilide and the carbonyl of another, and has a large degree of planarity in the 1,3-dicarbonyl moiety. For all compounds, the lowest triplet state (T_1) is calculated to have a geometry in which the azomethine bond is twisted by 70°−80° relative to the ground state, and to have a near-planar arrangement between the azomethine and the two carbonyl groups. The calculated lowest triplet energies are (in kcal/mol): 23.0 and 27.5 for two isomers of **1**, 25.2 for **2**, and 23.4 for **3**. The large geometrical differences between the ground and the lowest triplet states are proposed to provide an efficient mechanism for triplet state stabilization, and to stand at the origin of the observed nonadiabatic energy transfer in **1** and **2**. The presence of planarized equilibrium concentrations of **3** due to intramolecular H-bonding can explain the greater rates of energy transfer to **3** compared to **1** and **2**.

Introduction

Modern color photography has been based mostly on azomethine dyes, which are formed during processing by reaction between coated dye precursors and derivatives of *p*-phyenlenediamine (PPD) (Scheme 1).[1,2] As such, these dyes have become the subject of recent experimental,[3−5] and theoretical[6,7] investigations, aimed at understanding their spectral and photophysical properties.

We have been interested in studying aspects of the triplet states of azomethine dyes, such as their possible role in the mechanism of geometrical photoisometization about the azomethine double bond.[8] Because azomethine dyes do not phosphoresce or show singlet−triplet absorption in heavy atom solvents, their triplet energy has been determined using energy transfer techniques.[9] Unlike other classes of azomethine dyes, however, 1,3-dicarbonylazomethine dyes related to the compounds shown in Scheme 2 had shown behavior that could not be described uniformly by the conventional Sandros' vertical model for energy transfer.[10] The possibility of having a system of nonvertical energy transfer was thus raised, but no model was available at the time of the experiments to account for such condition. Sandros' analysis suggested the presence of a triplet species having an energy of 40 kcal/mol. This seemed reasonable in comparison with the triplet energy of other azomethine dyes. Pyrazolone azomethine dyes, for example, absorb near 540 nm, and have triplet energies near 25 kcal/mol. Since 1,3-dicarbonyl dyes absorb at wavelengths (λ_{max} = 420−440 nm) much shorter than the pyrazolone dyes, it is not unexpected for their triplet energies to be higher than the triplet energy of pyrazolone dyes. In a subsequent study, however, dyes related to **1** were found to quench singlet oxygen (triplet energy = 22.5 kcal/mol).[11] Although the quenching rates of singlet oxygen by

SCHEME 1: Formation of Azomethine Dyes in Color Photography[a]

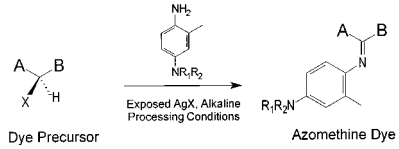

[a] A and B represent general substituents that can be part of a ring. X = H or anionic leaving group, R_1, R_2 = alkyl group.

SCHEME 2: Compounds Used in Energy Transfer Experiments

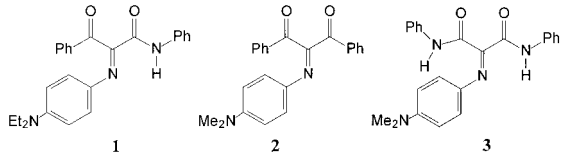

† Eastman Kodak Co. Current address: Department of Chemistry, Bowdoin College, 6600 College Station, Brunswick, ME 04011-8466. E-mail: fabu@bowdoin.edu.

‡ University of Rochester. E-mail: herkstroeter@chem.rochester.edu.

10.1021/jp002793h CCC: $20.00
Published on Web 01/26/2001

1 are slow, they still indicate that a triplet state with an energy much lower than 40 kcal/mol should be accessible to **1**.

In the past few years there have been several developments in the theory and application of energy transfer reactions. In the present study, previously reported data for the kinetics of energy transfer to **1** and **2** (Scheme 2), are analyzed using Balzani's model for nonvertical energy transfer.[12,13] To better understand this system, the energy profile of the related dye **3** has been determined. The new analysis shows that the observed kinetics in the given system can be consistent with formation of two distinct triplet states, T_1 and T_2, one having an energy close to 40 kcal/mol as previously estimated, and one having an energy in the proximity of 25 kcal/mol. In this analysis, formation of T_1 in **1** and **2**, but not in **3**, appears to take place in a mode having a large degree of nonadiabaticity. To elucidate the origin of these observations, density functional calculations have been carried out on the ground and the lowest triplet states of the given dyes. The results reveal that conformational flexibility available to the given dyes allows large structural and electronic changes to take place in the triplet state, providing thereby an efficient mechanism for triplet state stabilization, and possibly a unique condition for nonadiabatic energy transfer.

Results and Discussion

Background. In one version of an energy transfer experiment aimed at determining the unknown triplet energy of a compound (acceptor A), the rate constant (k_q^{ob}) for decay of a series of triplet donors ($^3D^*$) having known triplet energy (E_D) is measured in absence and at varying concentration of the acceptor.[14] The rate constant for energy transfer (k_q^{en}) from $^3D^*$ to A is then obtained according to the expression in Chart 1 (k_q^D is the intrinsic rate constant of decay of the triplet state of the donor in a particular solvent).

CHART 1: Determination of the Rate Constant for Energy Transfer from $^3D^*$ to A

$$D \xrightarrow{h\nu} {}^3D^*$$

$${}^3D^* \xrightarrow{k_q^D} D$$

$${}^3D^* + A \xrightarrow{k_q^{en}} D + {}^3A^*$$

$$k_q^{ob} = k_q^D + k_q^{en}[A]$$

Sandros' model relates k_q^{en} and the free energy of eq 1, ΔG, by the function in eq 2.[15]

$${}^3D^* + A \underset{k_{-d}}{\overset{k_d}{\rightleftharpoons}} [D\cdots{}^3A^*] \underset{k_d}{\overset{k_{-d}}{\rightleftharpoons}} D + {}^3A^* \qquad (1)$$

$$k_q^{en} = \frac{k_d}{1 + \exp\left(\frac{\Delta G}{RT}\right)} = \frac{k_d}{1 + \exp\left(\frac{E_A - E_D}{RT}\right)} \qquad (2)$$

When eq 1 is largely exergonic (negative ΔG), k_q^{en} is predicted to reach the diffusion-controlled limit, $k_q^{en} = k_d$ in eq 2. As ΔG becomes more positive, k_q^{en} becomes smaller. By equating ΔG to the triplet energy difference between D and A ($E_A - E_D$), the triplet energy of A (E_A) can be determined from the dependence of k_q^{en} on E_D in eq 2.

Balzani's model for energy transfer, eqs 3 and 4, is more comprehensive than Sandros'. In addition to the thermodynamics term, it incorporates two terms from conventional transition state theory in the expression of k_q^{en}, namely $\Delta G^{\ddagger}_0$ and k_q^0 (eq 4), for the standard free energy of activation and the preexponential factor for the forward energy transfer step in eq 3, respectively.[13]

TABLE 1: Energy of the Triplet Donors (kcal/mol) Used in Energy Transfer Experiments, and Values of Observed Quenching Rate Constants Used in Figure 1[a]

triplet donor[b]	energy of triplet donor	k_q^{en} 10^{-9} (M^{-1} s^{-1})[c] **1**	**2**	**3**
chrysene	57	1.5		
1,2,5,6-dibenzanthracene	52		2.9	3.3
1,2,3,4-dibenzanthracene	51	2.2	2.2	3.5
1,2-benzanthracene	47		1.7	2.4
benzanthrone	47	1.5	2.8	2.7
1,12-benzperylene	46		2.3	2.2
9,10-dimethyl-1,2-benzanthracene	44	1.7	1.4	2.0
anthracene	43	1.9		2.5
3,4-benzpyrene	42		1.1	
3,4,9,10-dibenzpyrene	40	1.3	1.1	1.8
5-methyl-3,4,9,10-dibenzpyrene	38	0.60	0.65	1.5
3,4,8,9-dibenzpyrene	34		0.063	
anthanthrene	34	0.10	0.029	1.1
naphthacene	29	0.093	0.017	0.96
pyranthrene	27	0.066	0.010	0.60
violanthrene	25		0.0027	0.14
isoviolanthrene	24		0.0017	0.051
$^1O_2$	22.5	0.0080		

[a] All values are for measurements in benzene except for quenching of $^1O_2$, which was measured in pyridine. Units of rate constants, k_q^{en}, are in M^{-1} s^{-1}. [b] References for the triplet energy of the donors of are given in ref 10. Based on several repeated measurements, an upper limit of the error in the given rate constants may be estimated as ±20%.

$${}^3D^* + A \underset{k_{-d}}{\overset{k_d}{\rightleftharpoons}} [{}^3D^*\cdots A] \underset{k_{-en}}{\overset{k_{en}}{\rightleftharpoons}} [D\cdots{}^3A^*] \underset{k_d}{\overset{k_{-d}}{\rightleftharpoons}} D + {}^3A^* \qquad (3)$$

$$k_q^{en} = \frac{k_d}{1 + \exp\left(\frac{\Delta G}{RT}\right) + \frac{k_{-d}}{k_{en}^0}\exp\left\{\frac{\Delta G}{RT} + \frac{\Delta G^{\ddagger}_0}{(\ln 2)RT}\ln\left[1 + \exp\left(-\frac{\Delta G \ln 2}{\Delta G^{\ddagger}_0}\right)\right]\right\}} \qquad (4)$$

Terms and Units: k_q^{en} is the rate constant for energy transfer (M^{-1} s^{-1}); ΔG is the free energy for eq 3 (kcal/mol); $\Delta G^{\ddagger}_0$ is the intrinsic free energy of activation of the forward energy transfer step in eq 3 (kcal/mol); k_d is the diffusion rate constant (M^{-1} s^{-1}); k_{en}^0 is the preexponential factor for formation of $[D\cdots{}^3A^*]$ (s^{-1}); and k_{-d} is the dissociation rate constant of $[D\cdots{}^3A^*]$ (s^{-1}).

k_{en}^0 relates to the reaction transmission coefficient, κ, which is a product of nuclear and electronic factors.[16,17] The nuclear factor allows for the possibility of tunneling in the system. The electronic factor has a spin statistical component and an orbital overlap component. When either the HOMO−HOMO or LUMO−LUMO overlap of the closed shell donor−acceptor pair is small, the overlap component will be reduced, and k_{en}^0 can get small enough that (k_{-d}/k_{en}^0) in eq 4 becomes greater than unity. In this case, the diffusion-controlled limit (k_d) is not reached even when the reaction is largely exergonic, and rates of energy transfer will acquire nonadiabatic character.[18,19]

Analysis of Energy Transfer Data. The triplet donors used in energy transfer experiments and their energies are given in Table 1, along with the rate constants for their quenching by **1**, **2**, and **3** in benzene (Scheme 2). All measurements were done by flash photoelectric techniques as described in details in ref

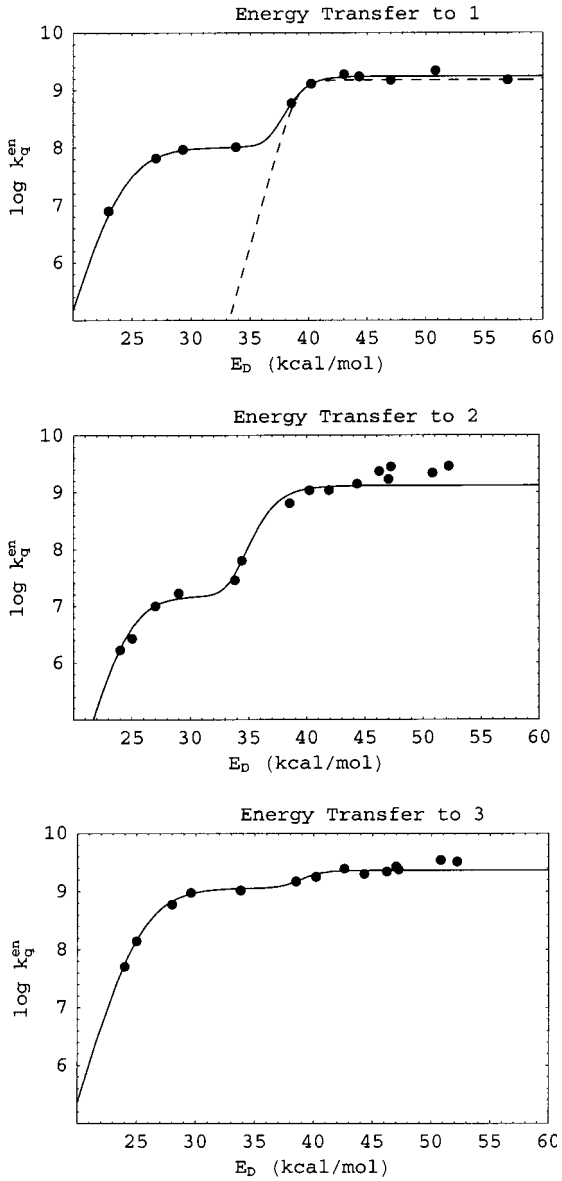

Figure 1. Energy transfer plots for the dyes in Scheme 2 (a (top) **1**; b (middle) **2**; c (bottom) **3**) and the measurements given in Table 1. Curves are for two Balzani functions defined by the parameters in Table 2.

10. Reference 10 also includes information about the synthesis and purification of the dyes, and references for the triplet donors.[20] Energy transfer plots are given in Figure 1, and the parameters used in curve fit are summarized in Table 2.

The dashed curve in Figure 1a is the theoretical Sandros plot (eq 2) for energy transfer from a series of triplet donors to an acceptor having a triplet energy EA = 39 kcal/mol. To achieve the given fit of the high-energy region by this curve, it was necessary to use a value of $k_d = 1.5 \times 10^9$ s^{-1} in eq 2, which is significantly smaller than the value of the theoretical diffusion-controlled rate constant (1.1×10^{10} s^{-1}, in benzene) predicted by Sandros' model for exergonic reactions. Clearly, functions derived from eq 2 cannot fit all the observed data of **1**. The same is true for energy transfer to **2** and **3** (Figure 1b,c). In discussing this result, we have argued against the possibility of complications due to electron or proton-transfer reactions, and raised the possibility of having nonvertical energy transfer.[10] Application of a single Balzani function (eq 4) to the given data, however, cannot accomplish more satisfactory fits. In particular, there seems to be an abrupt break in energy transfer

TABLE 2: Summary of the Plotting Parameters Used in Figure 1[a]

	1	**2**	**3**
E_{A1}	23.4 ± 1.6	23.4	25.0
$(k^0_{en})_1$	$1.2 \pm 0.5 \times 10^8$	1.5×10^7	1.5×10^9
$(\Delta G^{\ddagger}_0)_1$	1.3 ± 1.0	1.3	1.3
E_{A2}	38.5 ± 1.7	36.5	38.5
$(k^0_{en})_2$	$2.2 \pm 0.5 \times 10^9$	1.8×10^9	1.5×10^9
$(\Delta G^{\ddagger}_0)_2$	0.7 ± 0.9	1.0	0.75

[a] Parameters for **1** were obtained by nonlinear regression analysis for two functions of the form given in eq 4, with error limits given as the confidence interval (CI) at the 0.95 confidence level. The complete statistical report of the fit is given in the Supporting Information. Parameters for **2** and **3** were empirically adjusted to achieve the fits in Figures 1b and 1c, respectively. In all cases, values of 1.1×10^{10} M^{-1} s^{-1} and 1.27×10^{10} s^{-1} were used for k_d and k_{-d}, respectively. E_A and $\Delta G^{\ddagger}_0$ are in kcal/mol, k^0_{en} in s^{-1}.

rates near the donor energy of 35 kcal/mol, which divides the data into two subsets, thus precluding correct description by a single Balzani function. This behavior is distinct from that observed in other systems exhibiting extreme nonvertical energy transfer.[21,22] The observation of similar breaks in the energy profile of several 1,3-dicarbonyl dyes related to **1**, as well as in **2** and **3**, but in none of the other azomethine dyes studied by us[9,10] or by others,[23] suggests there is a physical basis for their appearance. Indeed, examples with stepping plateaus in rates of energy transfer are well-known in systems involving transition metal complexes.[24−26] These results have been interpreted in terms of formation of more than one triplet state in energy transfer reactions having different degrees of adiabaticity (different values of k^0_{en} in eq 4).[13] Making the hypothesis that energy transfer to the dyes considered in the present study produces more than one triplet species gives good fits to the observed data.

The solid curves in Figure 1 treat the observed k_q^{en} values as the sum of two rate constants, k_{q1} and k_{q2}, each having the form given in eq 4.[27] For **1** (Figure 1a), the fit was done by nonlinear regression analysis of all available data including the observed rate of quenching of singlet oxygen.[28] In this plot, k_{q2} represents formation of a triplet species (acceptor A2) with $E_{A2} = 38.6$ kcal/mol, in a reasonably adiabatic reaction, $(k^0_{en})_2 = 2.3 \times 10^9$ s^{-1}, having a small activation energy, $(\Delta G^{\ddagger}_0)_2 = 0.7$ kcal/mol. k_{q1} on the other hand, describes a reaction having significant nonadiabatic character, $(k^0_{en})_1 = 1.3 \times 10^8$ s^{-1}, and slightly larger intrinsic activation barrier $(\Delta G^{\ddagger}_0)_1 = 1.3$ kcal/mol, for formation of a triplet species with $E_{A1} = 23.4$ kcal/mol. If the measurement for singlet oxygen quenching, which was measured in pyridine, is discarded, only an upper limit of 25 kcal/mol can be obtained for E_{A1} by assuming $(\Delta G^{\ddagger}_0)_1 = 0.0$ kcal/mol.

For **2**, lack of sufficient measurements in the low-energy region, and data scatter in the high-energy region, preclude definitive fits to be made. The parameters for the curve in Figure 1b have been determined by using the E_{A1} and $(\Delta G^{\ddagger}_0)_1$ values found for **1** (23.4 and 1.3 kcal/mol, respectively), and adjusting the remaining until an acceptable fit was achieved for the measurements in the 25−45 kcal/mol energy range. This requires a value of $(k^0_{en})_1$ smaller than that found for **1** (1.5×10^7 s^{-1}, Table 2), and gives 36.5 kcal/mol and 1.8×10^9 s^{-1} for E_{A2} and $(k^0_{en})_1$, respectively. Overall, this set of empirical parameters can be varied only in a narrow range to retain acceptable fits in the specified energy range.

As is the case for **1** and **2**, the observed energy profile of **3** (Figure 1c) also shows two regions. However, the observed energy transfer rate constants in the low triplet energy region

of **3** are much greater than the corresponding rate constants for **1** and **2** in the same region (Table 2 and Figure 1c), and seems to be due to differences in the adiabaticity of the reaction. Indeed, an empirical fit of the observed data of **3** in the 25−45 kcal/mol energy range within the framework of the hypothesis adopted for energy transfer to **1** requires similar values of k_{en}^0 in the formation of the two proposed triplet states ($(k_{en}^0)_1 = (k_{en}^0)_2 = 1.5 \times 10^9$ s^{-1} for **3** in Table 2). In spite of this difference, the energies of the two triplet states of **3** obtained in Figure 1c ($E_{A1} = 25.0$ and $E_{A1} = 38.5$ kcal/mol) remain comparable to those obtained for **1** and **2** (Table 2).

In brief, the above analysis demonstrates that observed rates of energy transfer to the given 1,3-dicarbonylazomethine dyes can be consistent with formation of two triplet states, having energies near 25 and 40 kcal/mol. For **1** and **2** this analysis requires that the lowest triplet energy species be formed in a nonadiabatic step. In the known examples of nonadiabatic energy transfer in systems involving metal complexes, nonadiabaticity has been proposed to arise from shielding of the metal core orbitals from the orbitals of the donor or acceptor by the coordinated ligands. Recently, Balzani et al. and Deshayes et al. have independently developed a novel approach for introducing nonadiabaticity in the quenching of triplet biacetyl by organic acceptors, by imprisoning biacetyl within the walls of a hemicarcerand.[29,30] As will be shown in the computational study, the condition for nonadiabaticity in 1,3-diacarbonyl azomethine dyes is likely to arise from unique conformational differences between their ground and lowest triplet states.

Computational Methods. All calculations were carried out using Gaussian 94.[31] Geometries and energies have been obtained by the B3LYP or UB3LYP[32] methods with the 6-31G* basis set.[33] Zero-point energy and thermal excitation terms were estimated from normal-mode analysis calculations carried out at the HF/3-21G or ROHF/3-21G level of theory, using frequencies scaled by 0.92, and $T = 298.15$ K. For both the vertical and minimized triplet states, the UB3LYP wave functions showed no spin contamination ($\langle s^2 \rangle \approx 2.0$). A recent investigation of Z/E isomerization of polyenes by Ottoson et al. has shown that DFT methods (UB3LYP/6-31G**) comparable to the one used in our present study give vertical and relaxed triplet energies that are close to experimental values, and that are comparable to results from high level ab initio methods.[34] Solvation effects on the geometries and energetics of **1** were briefly examined using the continuum self-consistent reaction field model (SCRF) of Onsager, with benzene as solvent. The radius of the solute required in these calculations was obtained from "volume" calculations at the B3LYP/6-31g* level and the gas phase equilibrium geometries. The schematic molecular orbital diagrams used in discussing the electronic structure of the calculated species in the present study are qualitative and are based on displays by the Cerius molecular modeling system.[35] Atomic spin densities were calculated using the natural orbital scheme of Reed and Weinhold.[36] Cartesian coordinates of the minimized geometries are given as Supporting Information. Calculated ground and lowest triplet state energies are collected in Table 3.

Geometry and Electronic Structure of the Ground and the Lowest Triplet States. Both isomers defined by the azomethine double bond have been considered in calculating the ground-state geometry of **1** (**1**a-S_0 and **1**b-S_0, Scheme 3). At the B3LYP/6-31g* level of theory, **1**a-S_0 is calculated to be 1.4 kcal/mol lower in energy than **1**b-S_0, or 2.7 kcal/mol when the ZPE and thermal excitation terms are accounted for (ΔG in Table 3). Several attempts to locate additional minima of **1** by energy minimization starting with twisted variations of these two isomers converged back to either one of them.

TABLE 3: Calculated Ground and Lowest Triplet State Energies

molecule	total E (B3LYP/6-31G*) (au)	rel E (B3LYP) (kcal/mol)	ZPE[a] (HF) (kcal/mol)	rel G[b] (B3LYP, HF) (kcal/mol)
1a-S_0	−1243.109 070	0.0	263.9	0.0
1b-S_0	−1243.106 905	1.4	264.3	2.7
1a-T_1	−1243.059 772	30.9	262.1	27.5
1b-T_1	−1243.069 560	24.8	262.8	23.0
1c-T_1	−1243.055 714	33.5		
1a-S_0-**S**[c]	−1243.110 857	0.0		
1b-S_0-**S**[c]	−1243.108 028	1.8		
1a-T_1-**S**[c]	−1243.063 048	30.0		
1b-T_1-**S**[c]	−1243.073 233	23.6		
2-S_0	−1187.731 326	0.0	252.6	0.0
2a-T_1	−1187.687 684	27.4	251.9	25.4
2b-T_1	−1187.682 742	30.5		
3-S_0	−1298.485 192	0.0	275.9	0.0
3-T_1	−1298.442 150	27.0	273.8	23.4
H-S_0	−938.053 997	0.0		
H-T_1	−937.993 431	39.2		

[a] ZPE calculated at the HF/3-21G or ROHF/3-21G level using frequencies scaled by a factor of 0.92. [b] Relative G corresponds to B3LYP/6-31g*. Energies plus thermal free energy correction terms calculated at 25 °C using the scaled 3-21G frequencies. [c] Energies for geometries minimized in a benzene solvent electric dipole continuum (self-consistent reaction field calculations with the Onsager model).

SCHEME 3: Calculated Geometry of 1a-S_0 and 1b-S_0

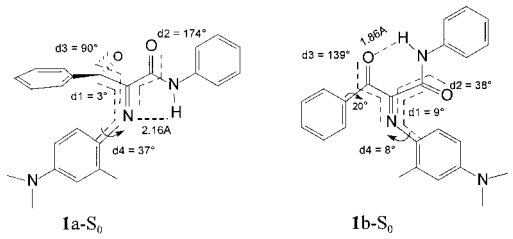

1a-S_0 **1**b-S_0

The geometry of **1**a-S_0 can be described in terms of two orthogonal planes, one containing the azomethine double bond and the anilide fragment (d1 = 174°), and one including the phenyl ketone group (d3 = 90°, Scheme 3). The anilide proton in this geometry is in close proximity of the azomethine nitrogen (2.16 Å) and may be viewed as forming a side-on intramolecular H-bond with the azomethine nitrogen.[37] The *p*-phenylenediamine ring, PPD, is rotated by 37° out of the azomethine−anilide plane (d4, Scheme 3). These parameters change only slightly when **1**-S_{0a} is minimized in a benzene solvent continuum. Specifically, the equilibrium d1, d3, and d4 angles calculated in a benzene continuum are 175°, 95°, and 30°, respectively. These conformational details agree well with the crystallographically determined molecular structure of several 1,3-dicarbonyl azomethine dyes related to **1**.[38] This conformational mode is similar to that observed in some α, α′-tricarbonyl compounds.[39]

In **1**b-S_0, the minimized gas phase geometry exhibits an intramolecular H-bond between the anilide proton and the carbonyl of the phenyl ketone. At the equilbrium geometry of this isomer, each carbonyl is rotated by approximately 40° from the azomethine double bond (d2 and d3, Scheme 3), and the bond between the PPD ring and the azomethine nitrogen is substantially moved out of the azomethine plane (d1 = 9°). In addition, the ketone fragment shows nonplanar phenyl−carbonyl orientation (d5 = 20°, Scheme 3). These distortions suggest that the conformation required to effect the apparently favorable H-bond in **1**b-S_0 introduces greater steric repulsions in the

SCHEME 4: Calculated Distribution of the HOMO and LUMO in 1a-S_0

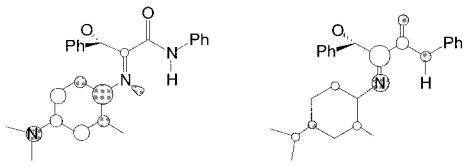

molecule, which makes **1**b-S_0 higher in energy than **1**a-S_0. It is very likely, however, that the gas phase calculations will overestimate the importance of intramolecular hydrogen bonding. When the calculations are done in a benzene continuum, the energy difference between **1**a-S_0 and **1**b-S_0 is 1.8 kcal/mol, compared to 1.4 kcal/mol in the gas phase (Table 3).

Analysis of the frontier molecular orbitals in **1**a-S_0 reveals that the highest occupied and lowest unoccupied MOs are primarily π-type orbitals (Scheme 4). The HOMO is calculated to be distributed mainly over the PPD ring and corresponds roughly to the out-of-phase combination between the highest occupied π-MO of the aromatic ring and the nonbonding electron pair of the amine. The HOMO also includes minor π (C) and σ (N) components from the azomethine atomic orbitals. The mixing of the σ (N) orbital and the π moiety is possible due to the twist of the PPD ring out of the azomethine plane (d4 = 37°; Scheme 3).

The LUMO in **1**a-S_0 is calculated to be localized on the azomethine−carbonyl−amide fragment, away from the fragment containing the HOMO, and corresponds effectively to one of the π-combinations of the planar azomethine−carbonyl fragment, which is mostly concentrated on the methine carbon. Due to the orthogonal orientation of the phenyl ketone relative to this fragment, the LUMO in **1**a-S_0 has no contribution from the carbonyl π-moiety of the ketone. One known property consistent with the geometry and electronic structure calculated for **1**a-S_0 is the observed striking near-independence of the lowest electronic absorption band to substitution on the phenyl ketone. NO_2 or NH_2 substituents at the para position of the phenyl ketone ring, for example, have hardly any effect on the λ_{max} of 422 nm and effect little or no shifts to 420 and 422 nm, respectively (cyclohexane).[40]

As would be expected from the HOMO and LUMO in Scheme 4, the vertical triplet state of **1**a-S_0, obtained by single-point triplet calculation on the ground state geometry, corresponds to promotion of an electron from the HOMO to the LUMO. No spin density is calculated on the twisted carbonyl group in the vertical triplet state of **1**. At the UB3LYP/6-31G* level of theory, the calculated gas phase vertical triplet energy of **1**a-S_0 is 55 kcal/mol and remains the same when calculated in a benzene continuum. This value is not unreasonable for the given dye, considering it absorbs at 422 nm (in benzene), which amounts to a vertical singlet energy of 68 kcal/mol. Energy minimization on the lowest triplet potential energy surface (T_1) starting with the ground state geometry of **1**a-S_0 affords **1**a-T_1 (Scheme 5) with two major conformational changes. First, the azomethine double is calculated to become twisted relative to the ground state: d1 = 68° (**1**a-T_1) vs 3° (**1**a-S_0). This is similar to the twist characterizing the lowest triplet states of olefins, azo, and azomethine compounds.[41] The other conformational modification leading to the relaxed triplet geometry is unique to the given system as it involves increased planarity of the ketone carbonyl with the azomethine bond: d3 = 28° (**1**a-T_1) vs 90° (**1**a-S_0). Similar conformational changes are also calculated upon triplet minimization starting with the geometry

SCHEME 5: Calculated Triplet State Geometry of 1a-T_1, 1b-T_1, and 1c-T_1

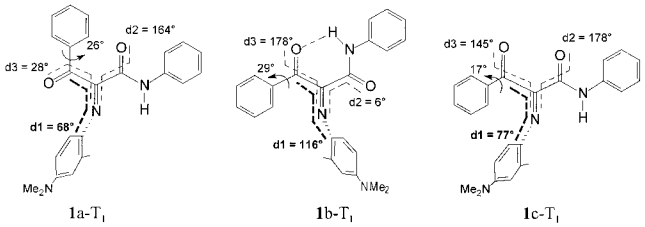

SCHEME 6: Comparison of Calculated Bond Distances in 1a-S_0 and 1a-T_1, Distribution of the Singly Occupied MOs in 1a-T_1, and Atomic Spin Density Values

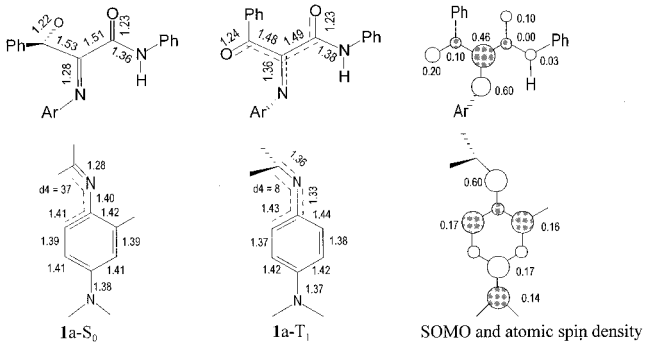

of **1**b-S_0. In this case, the two carbonyls in the product, **1**b-T_1, are basically coplanar with the azomethine bond (d2 = 6°, and d3 = 178°, Scheme 6). In both **1**a-T_1 and **1**b-T_1, the azomethine twist puts the two unpaired electrons in roughly two orthogonal fragments, thus giving formally an a″ state.

The relaxation energy for minimization of the vertical triplet state of **1**a-S_0 is 24.0 kcal/mol. This brings the relative energy of **1**a-T_1 to 30.9 kcal/mol above **1**a-S_0, or 27.5 kcal/mol after addition of the thermal terms (Table 3). Adding a benzene dipole continuum in the calculation does not change these values. The magnitude of the calculated relaxation energy for this dye is large and uncommon. However, it can be readily accounted for in terms of an efficient relaxation mechanism available to **1** through the two conformational changes mentioned above. Based on the HOMO and LUMO of **1**a-S_0 (Scheme 4), vertical triplet excitation can be viewed qualitatively as generating a local cation radical on the PPD fragment and an anion radical on the azomethine−carbonyl moiety. Scheme 6 compares calculated bond distances in these fragments in **1**a-S_0 and **1**a-T_1, and includes schematic representations of the singly occupied molecular orbitals (SOMO) in **1**a-T_1 along with major atomic spin density values.

Consistent with the in-phase−out-of-phase composition of the HOMO and LUMO in **1**a-S_0, Scheme 6 shows that geometry relaxation of the vertical triplet state results in increased alternation in the PPD fragment, an increase in the azomethine double bond, and a decrease in C−C bond distance between the methine and amide carbonyl. These skeletal changes do not require conformational modification to become effective, and can be approximately reproduced by partial minimization with all the angles and dihedrals frozen at the ground state values. The latter procedure gives a triplet relaxation energy of 8 kcal/mol. The two conformational changes that take place in **1**a-T_1 can bring additional stabilization in two ways. First, twist of the azomethine bond is expected to reduce the $\pi-\pi$ repulsion between the two unpaired electrons, and to reduce the effect of charge separation by allowing a kind of π-back-donation from

SCHEME 7: Calculated Geometry of the Ground and Lowest Triplet State of H-S_0 and H-T_1 (Bond Distances in Å)

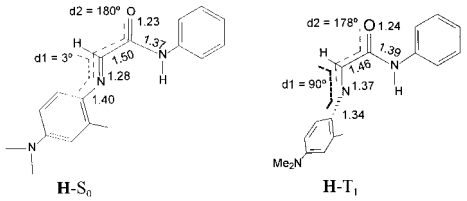

H-S_0 **H**-T_1

SCHEME 8: Comparison of Calculated Bond Distances (Å) in 1b-S_0 and 1b-T_1, Distribution of the Highest Singly Occupied MO in 1b-T_1, and Atomic Spin Density Values

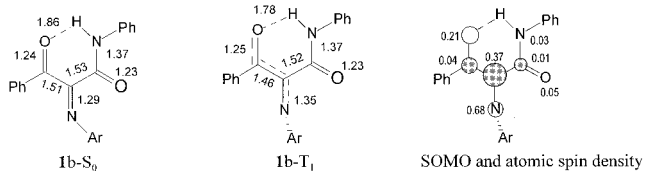

1b-S_0 1b-T_1 SOMO and atomic spin density

the lone pair of the azomethine nitrogen to the formally ionized PPD ring. Rotation of the phenyl ketone, on the other hand, provides additional stabilization by extending delocalization of the higher energy unpaired electron onto the keto carbonyl, as evident in the calculated spin density on the keto carbonyl in **1**a-T_1 (0.3 e^-). The effect of spin delocalization is also reflected in a decrease in the CC bond distance between the keto carbonyl and the methine carbon, from1.53 Å in **1**a-S_0 to 1.48 Å in and **1**a-T_1 (Scheme 6). In accord with the introduction of double bond character in this bond, it has been possible to calculate the geometrical isomer related to **1**a-T_1 by rotation of the phenyl ketone by 180° (**1**c-T_1 Scheme 5). The energy of **1**c-T_1 is calculated to be 2.5 kcal/mol higher in energy than **1**a-T_1 (Table 3).

In an attempt to separate the relative importance of the two conformational changes discussed above on the triplet relaxation energy, additional calculations were carried out on the ground (**H**-S_0) and triplet (**H**-T_1) states of the model molecule shown in Scheme 7.

The HOMO and LUMO in **H**-S_0 are similar to those shown in Scheme 4 for **1**a-S_0. Consistently, the vertical triplet energies of **H**-S_0 and **1**a-S_0 are calculated to be comparable: 57 and 55 kcal/mol, respectively. Minimization of the vertical triplet state of **H**-S_0 induces twist and geometrical changes in the azomethine-PPD fragment parallel to those that occur in **1**a-S_0, and affords a relaxation energy of 17.8 kcal/mol. This value is still large, but relaxation energies of comparable magnitudes are known.[42] The greater relaxation energy in **1**a-S_0 may hence be attributed to the contribution of the ketone group in spin delocalization.

Unlike the case in the ground state, the isomer with an intramolecular H-bond in the triplet state, **1**b-T_1 in Scheme 5, is calculated to be 6.1 kcal/mol lower in energy than **1**a-T_1, or 4.5 kcal/mol after adding the vibrational and thermal terms (Table 3). This is most likely the consequence of increased strength of the H-bond in the triplet state, brought by relief of steric effects upon twist of the azomethine bond, and by increase of the H-bond accepting properties of the keto oxygen due to delocalization of the higher energy unpaired electron on the keto carbonyl. Scheme 8 compares the geometric parameters of the azomethine-dicarbonyl fragment in **1**b-S_0 and **1**b-T_1. The increased effectiveness of H-bonding in the triplet state is apparent in the shorter H-bond in **1**b-T_1 (1.78 Å).

SCHEME 9: Calculated Geometry of the Ground and Lowest Triplet States of 2

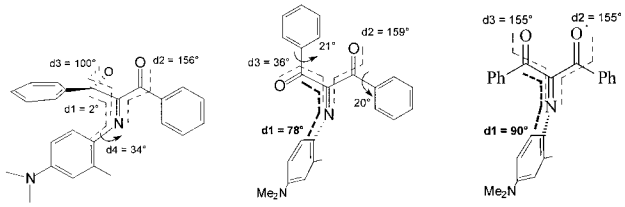

2-S_0 **2a**-T_1 **2b**-T_1

SCHEME 10: Calculated Geometry of the Ground and Lowest Triplet State of 3

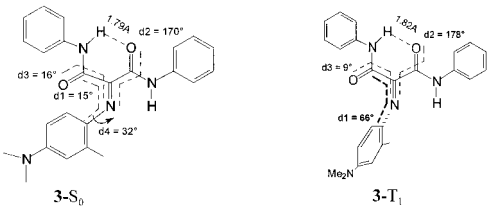

3-S_0 **3**-T_1

For **2**, only one isomer can be defined against the azomethine double bond. In the calculated ground state equilibrium geometry of this dye (**2**-S_0, Scheme 9), both carbonyls are moved out of the azomethine plane (d2 = 156° and d3 = 100°). In this arrangement, the HOMO and LUMO are calculated to be closely related to those in **1**a-S_0 (Scheme 4), and continue to lack any contribution from the π-orbitals of the carbonyl defined by d3 in Scheme 9. Minimization of the triplet state starting with the geometry of **2**-S_0 affords **2a**-T_1, with planarity between the two carbonyls (d2 = 159°, d3 = 36°, Scheme 9).

The calculated vertical triplet energy of **2**-S_0 is 49 kcal/mol, significantly smaller than vertical triplet energy of **1**a-S_0 (55 kcal/mol). An indirect support for this ordering may be obtained from the observed difference in the electronic absorption spectra of these dyes: λ_{max} = 420 or 448 nm, for **1**a-S_0 and **2**-S_0, respectively (in benzene), which affords 4.2 kcal/mol for the difference of their vertical singlet excitation energy. After geometry minimization, the relaxed triplet energy of **2a**-T_1 is calculated to be 25.2 kcal/mol above the energy of **2**-S_0 (Table 3). The symmetric isomer **2b**-T_1 (Scheme 9) minimized in the C_s point group is calculated to be 3.1 kcal/mol above **2a**-T_1 (Table 3).

The calculated equilibrium geometries of the ground and lowest triplet states of **3**, **3**-S_0 and **3**-T_1, respectively, are given in Scheme 10. Both geometries exhibit an intramolecular H-bond, and both show a nearly planar carbonyl−azomethine moiety. The presence of two amide groups in **3** seems to make intramolecular H-bonding in the ground state of **3** less hindered than in the case of **1**b-S_0. It is noted that unlike the case of **1**b-S_0, formation of an intramolecular H-bond with the amide carbonyl in **3**-S_0 retains the side-on intramolecule hydrogen bond between an anilide proton and the azomethine nitrogen.

The HOMO in **3**-S_0 is calculated to be similar to the HOMO of **1**a-S_0 (Scheme 4). As a result of the large planarity among the azomethine−carbonyl groups in **3**-S_0 (d1 = 15°, Scheme 10), however, the LUMO in **3**-S_0 is calculated to be delocalized on both carbonyls. Consistently, **3**-S_0 is calculated to have a much lower vertical triplet energy than **1a**-S_0 (41 vs 55 kcal/mol). In solvents having potential hydrogen-bond acceptor atoms such as ethyl acetate, THF, and acetonitrile, the shape of the lowest energy absorption band of **1** and **3** is similar (Figure 2). This result does not support the presence of intramolecular

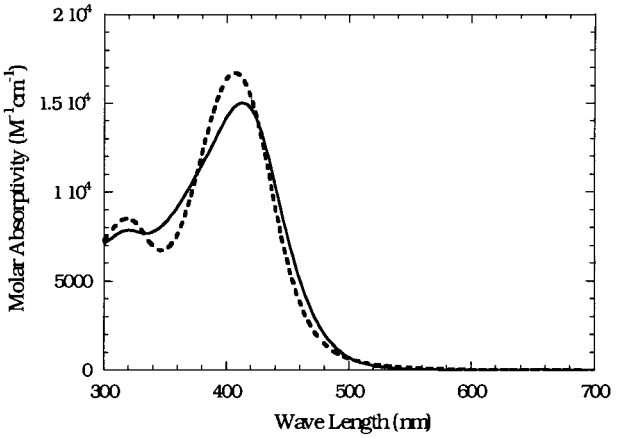

Figure 2. Measured spectra of **1** (solid line) and **3** (dotted line) in ethyl acetate (25 °C). Approximately 1 mM solutions in 1 mm cells.

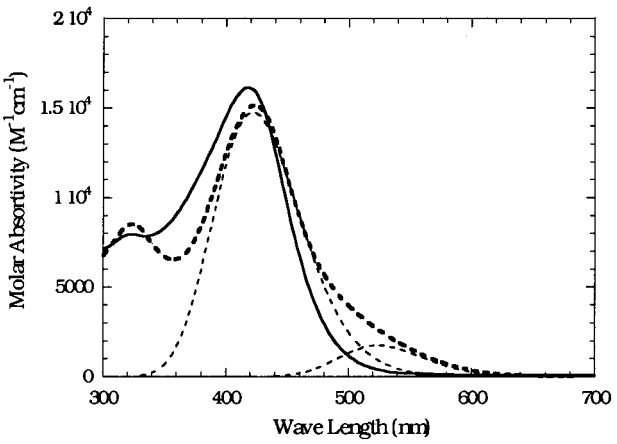

Figure 3. Measured spectra of **1** (solid line) and **3** (bold dotted line) in benzene (25 °C). Approximately 1 mM solutions in 1 mm cells. Normal dotted lines are the fitted components of **3**, obtained by deconvoluting the measured spectrum in the wavenumber domain using Gaussian functions.

H-bonding in **3**, but rather suggests that **1** and **3** have similar conformations in these solvents. In benzene, the intensity and shape of the peak of **1** is comparable to that in ethyl acetate (Figures 2 and 3). For **3**, on the other hand, the benzene spectrum (Figure 3) exhibits two peaks in the visible region: one with λ_{max} at 420 nm that is similar to the spectrum in ethyl acetate but with lower intensity, and a new broad absorption band with λ_{max} at 530 nm. The ratio of the areas of the 530 nm to the 420 nm peaks is 0.07, and remains unchanged in the concentration range between 0.05 and 1.0 mM. The observed spectra of **1** and **3** in methylene chloride are similar to those observed in benzene. In cyclohexane **3** has two peaks in the visible region that are of comparable intensities.[43] The sum of the areas of the two visible peaks of **3** in benzene or cyclohexane is close to the area of the visible peak in ethyl acetate (integration done in the wavenumber domain). These observations are consistent with the presence of an equilibrium between two monomeric species of **3** in these solvents: one having a geometry similar to that of **1**, and one matching the calculated structure exhibiting intramolecular H-bond with a carbonyl (Scheme 9). The NMR spectra of **1** and **3** are also supportive of this interpretation.[44] The energy difference between the excitation energies of the two peaks of **3** in benzene (14 kcal/mol) is remarkably similar to the calculated difference between the vertical triplet energies of **1** and **3**. Attempts to locate a minimum on the ground state energy surface of **3** that does not have an intramolecular H-bond with the carbonyl have not been successful. In the absence of solvent, it is likely that intramolecular H-bonding will be strongly favored over the twisted conformation. It is noted that the two proposed species of **3** are related by rotation around a CC bond having largely single bond character. Thus no significant barrier is expected for their interconversion.

Finally, the calculated energy difference between the ground and triplet states of **3** is 23.4 kcal/mol (Table 3), a value close to that inferred from the energy transfer experiments in Figure 1c (E_{A1} = 25.0 kcal/mol, Table 2).

Origin of the Nonadiabatic Energy Transfer. Considering the large structural and electronic differences between the ground and lowest triplet states of **1** and **2**, it is not unreasonable for the kinetics of their triplet formation by energy transfer to acquire some degree of nonadiabaticity. For these dyes, the necessary requirement for nonadiabaticity seems to be provided in the involvement of the twisted phenyl ketone group, since the carbonyl orbitals of this group are isolated from the HOMO and LUMO in the ground state, but are principal in spin accommodation in the relaxed triplet state. Support for this interpretation is provided by the reduced nonadiabatic character of energy transfer to **3**. In benzene, the spectrum of **3** indicates the presence of a significant equilibrium amount of a species having intramolecular H-bonding. Unlike the case in **1** and **2**, the calculations show that such species should have a large degree of planarity between the two carbonyls with the consequence of delocalizing the LUMO over the two carbonyls in the ground state. In simplistic terms, this geometry of **3** is more prepared for triplet exchange than either **1** or **2**.

For **1**, the calculations predict that **1**b-T_1 should be the lowest energy isomer in the triplet state (Table 3). Formation of **1**b-T_1 by energy transfer to **1**a-S_0, however, will require an approximately 180° rotation of the anilide moiety in addition to the azomethine twist and the rotation of the ketone group, which are unlikely to take place in a concerted single step. In addition, the lower energy of this isomer may be overestimated by the gas phase calculations. Thus, to interpret the quenching profile of **1** in Figure 1a, it seems more reasonable to attribute the lower energy region to formation of **1**a-T_1 rather than to **1**b-T_1. The similarity of the energy profiles of **1** and **2** (Figure 1, a and b) is consistent with this interpretation.

Nature of the Higher Energy Triplet Species. Attempts to identify a minimum on the lowest triplet potential energy surface (T_1) of the given dyes that would match the higher energy triplet species proposed in analysis of rates of energy transfer have not been successful. A torsion angle drive search on the UB3LYP/6-31G* T_1 surface of a dye related to **1** by replacement of the keto and amide phenyl groups by methyl groups, for example, revealed that in the region of the untwisted azomethine bond (d1 = 0°, Scheme 3), the T_1 surface corresponds to a transition state for twist of this bond. This suggests that the higher energy triplet species proposed in energy transfer experiments is an excited triplet state, belonging to the T_2 potential energy surface. The presence of several functional groups containing π-orbitals and lone electron pairs in the given dyes allows for several excited states such as carbonyl or azomethine $n \rightarrow \pi^*$ and $\pi \rightarrow \pi^*$ states. It is not unlikely for the relaxed energies of such excited states (T_2, T_3, etc.) to be closely spaced. The energy range in which excited triplet states are proposed in Figure 1 is fairly wide (40−55 kcal/mol) and may actually involve more than one type of excited state (T_2, T_3, etc.). Due to their large size and lack of symmetry, application of levels of theory appropriate to address the issue

of the excited triplet states of the given dyes is beyond the scope of the present study.

Conclusions

The new analysis of energy transfer to the given 1,3-dicarbonyl azomethine dyes leads to two major findings. First, the analysis puts the energy of the lowest triplet state of these dyes in the vicinity of 24 kcal/mol. Density functional calculations support this result and provide an explanation for their seemingly low values. The energy of the lowest triplet state of dyes is among the important parameters in understanding their photochemistry. This state can undergo, for example, energy and electron transfer reactions with surrounding molecules, such as a dye in its ground state or molecular oxygen.[45] The energetics of such reactions depend strongly on the triplet energy of the dye. The low estimates of the triplet energy of the given dyes should have great implications in interpreting the role of the triplet state in their photochemistry.

Our second finding is that formation of the lowest triplet states of **1** and **2** by energy transfer appears to follow a largely nonadiabatic step. Previously known systems of nonadiabatic energy transfer have involved either transition metal coordination complexes, or systems in which the energy donor has been separated from the acceptor by incorporating it in a molecular cage. The computational investigation suggests that the condition for nonadiabatic behavior in **1** and **2** is provided by unique conformational differences between the geometry of the ground and the lowest triplet states. The conformation of the ground state of **1** and **2** isolates the orbitals of one of the two carbonyls from the HOMO and the LUMO of the dye. In the triplet state, the conformation changes, and the initially isolated carbonyl becomes important in accommodating spin. Support for this proposition is provided by the behavior of **3**. Intramolecular H-bonding in this dye drives a conformation in which the two carbonyl groups have a large degree of planarity in the ground state, disrupting thus the condition for nonadiabatic behavior proposed for **1** and **2**. Accordingly, **3** is found to undergo energy transfer reactions at rates much greater than **1** or **2**.

Acknowledgment. Thomas Welter is thanked for synthesizing the dyes used to make new spectroscopic and kinetics measurements. John Baloga, Samir Farid, and Michael Youngblood are acknowledged for helpful discussion. Todd Beverly is thanked for administering computer hardware and software resources.

Supporting Information Available: Cartesian coordinates of calculated geometries, and a statistical report from the nonlinear regression fit used in Figure 1a. This material is available free of charge via the Internet at http://pubs.acs.org.

References and Notes

(1) Kapecki, J.; Rodgers, J. Color Photography. In *Kirk-Othmer Encyclopedia of Chemical Technology*, 4th ed.; John Wiley and Sons: New York, 1993; Vol. 6.

(2) (a) James. T. H., Ed. *Theory of the Photographic Process*, 4th ed.; Macmillan Publishing Co.: New York, 1978. (b) Carroll, B. H.; Higgins, G. C.; James, T. H. *Introduction to Photographic Theory: the Silver Halide Process*; Wiley: New York, 1980.

(3) (a) Wilkinson, F.; Worrall, D.; McGarvey, D.; Goodwin, A.; Langley, A. *J. Chem. Soc., Faraday Trans.* **1993**, *89*, 2385−90. (b) Wilkinson, F.; Worrall, D. R.; Chittock, R. S. *Chem. Phys. Lett.* **1990**, *174*, 416−22.

(4) (a) Berry, R. J.; Douglas, P.; Garley, M. S.; Jolly, T.; Clarke, D.; Moglestue, H.; Walker, H.; Winscom, C. *J. Photochem. Photobiol., A* **1999**, *120*, 29−36. (b) Douglas, P.; Townsend, S. M.; Booth, P. J.; Crystall, B.; Durrant, J. R.; Klug, D. R. *J. Chem. Soc., Faraday Trans.* **1991**, *87*, 3479−85.

(5) (a) Zdzislaw, Z.; Ilona, P.; Bronislaw, M.; Gordon, L. H.; Jerzy, P. *J. Chem. Soc., Perkin Trans.* 2 **1999**, *10*, 2147−2154. (b) Zdzislaw, K.; Marek, P.; Jerzy, P. *Chem. Mater.* **1998**, *10*, 3555−3561.

(6) Kondakov, D. "Excited singlet states of pyrazolotriazole azomethine dyes: are they hot? Theory and experiment." Presented at the 219th ACS National Meeting, 2000, San Francisco, CA.

(7) (a) Friedrich, L. E.; Eilers, J. E. *J. Imaging. Sci. Technol.* **1994**, *38*, 24−7. (b) Adachi, M.; Murata, Y. *J. Phys. Chem. A* **1998**, *102*, 841−845. (c) Adachi, M.; Murata, Y.; Nakamura, S. *J. Am. Chem. Soc.* **1993**, *115*, 4331−8. (d) Heinz, M.; Lothar, H.; Horst, W. *Z. Chem.* **1989**, *29*, 66−7.

(8) (a) Herkstroeter, W. G. *Mol. Photochem.* **1971**, *3*, 181−91. (b) Asano, T.; Okada, T.; Herkstroeter, W. G. *J. Org. Chem.* **1989**, *54*, 379−83. (c) Herkstroeter, W. G. *J. Am. Chem. Soc.* **1973**, *95*, 8686.

(9) Herkstroeter, W. G. *J. Am. Chem. Soc.* **1976**, *98*, 330.

(10) Herkstroeter, W. G. *J. Am. Chem. Soc.* **1975**, *97*, 3090.

(11) Smith, W. F., Jr.; Herkstroeter, W. G.; Eddy, K. L. *J. Am. Chem. Soc.* **1975**, *97*, 2764.

(12) Balzani, V.; Bolletta, F. *J. Am. Chem. Soc.* **1978**, *100*, 7404.

(13) Balzani, V.; Bolletta, F.; Scandola, F. *J. Am. Chem. Soc.* **1980**, *102*, 2152.

(14) Lamola, A. A.; Turro, N. J. Energy Transfer and Photochemistry. In *Techniques of Organic Chemistry*; Leermakers, P. A., Evans, T. R., Eds.; Interscience Publishers: New York, 1969.

(15) Sandros, K. *Acta Chem. Scand.* **1964**, *18*, 2355.

(16) The conventional transition state theory expression for the rate constant of the forward reaction in eq 3 can be written as: $k_q^{en} = k_{en}^0 \exp(-\Delta G^{\ddagger}/RT)$, where $k_{en}^0 = \kappa(\mathbf{k}T/h)$, κ accounts for the possibility that the activated complex (transition state) will give the reactants back, rather than the products. For discussion, see chapter 4 in Laidler, K. J. Chemical Kinetics.

(17) Laidler, K. J. *Chemical Kinetics*, 3rd ed.; Harper and Row: Publishers: New York, 1987.

(18) The term "nonadiabatic" is used in this study in a generic sense to denote a reaction having rate constant with a small preexponential value, in a way similar to that adopted by Balzani. For a discussion on the use of the term in reaction kinetics see Laidler in the next reference.

(19) Laidler, K. J. *Can. J. Chem.* **1994**, *72*, 936.

(20) The registry numbers of **1** and **2** are 4754-92-1, and 4755-00-4, respectively. **3** is a new compound and was prepared by a similar way as described for **1** and **2** in ref 10.

(21) (a) Gorman, A. A.; Hamblett, I.; Rushton, F. A. P.; Unett, D. J. *J. Chem. Soc., Chem. Commun.* **1993**, *12*, 983. (b) Gorman, A. A.; Hamblett, I.; Rushton, F. A. P.; Unett, D. J. *J. Chem. Soc., Chem. Commun.* **1993**, *12*, 983. (c) Caldwell, R. A.; Riley, S. J.; Gorman, A. A.; McNeeney, S. P.; Unett, D. J. *J. Am. Chem. Soc.* **1992**, *114*, 4424.

(22) Brennan, C. M.; Caldwell, R. A.; Elbert, J. E.; Unett, D. J. *J. Am. Chem. Soc.* **1994**, *116*, 3460.

(23) (a) Douglas, P. *J. Photogr. Sci.* **1988**, *36*, 83. (b) Douglas, P.; Townsend, S. M.; Ratcliffe, R. *J. Imaging Sci.* **1991**, *35*, 211.

(24) (a) Wilkinson, F.; Tsiamis, C. *J. Phys. Chem.* **1981**, *85*, 4153−7. (b) Wilkinson, F.; Tsiamis, C. *J. Chem. Soc., Faraday Trans. 2* **1981**, *77*, 1681−93. (c) Wilkinson, F.; Tsiamis, C. *J. Am. Chem. Soc.* **1983**, *105*, 767−74. (d) Wilkinson, F.; Tsiamis, C. *Inorg. Chem.* **1984**, *32*, 3571−7.

(25) Hug G. L.; Marciniak B. *J. Phys. Chem.* **1994**, *98*, 7523−7532.

(26) For reviews of energy transfer to metal complexes see: (a) Bronislaw, M.; Buono-Core, G. E. *J. Photochem. Photobiol., A* **1990**, *52*, 1−25. (b) Bronislaw, M.; Buono-Core, G. E. *Coord. Chem. Rev.* **1990**, *99*, 55−87.

(27) The plots were made using the calculated values of k_d and k_{-d}. k_d is given by the Debye equation: $k_d = 8RT/3\eta$, where η is the solvent viscosity (Laidler (ref 17), Chapter 6). For benzene at 25°, $\eta = 6.0 \times 10^{-4}$ kg m^{-1} s^{-1}, and $k_d = 1.1 \times 10^{10}$ M^{-1} s^{-1}. k_d and k_{-d} are related by the Eigen equation: $k_{-d} = k_d(3000)/(4\pi N r^3)$, where N is Avogadro's number and r is the effective radius of the encounter complex in eq 3 (Eigen, M. *Z. Phys. Chem.* (*Frankfurt am Main*) **1942**, *1*, 265. All determinations of k_{-d} in this study were done using $r = 7.0 \times 10^{-8}$ m, affording $k_{-d} = 1.28 \times 10^{10}$ M^{-1} s^{-1}. Using different values of r in calculating k_{-d} has a small effect on the magnitude of $(k_{en}^0)_1$ and $(k_{en}^0)_2$ in data fitting, but does not change the conclusions of the study.

(28) Nonlinear regression was done using Mathematica V.3.0.1.

(29) (a) Farran, A.; Deshayes, K. D. *J. Phys. Chem.* **1996**, *100*, 3305. (b) Place, I.; Farran, A.; Deshayes, K.; Piotrowiak, P. *J. Am. Chem. Soc.* **1998**, *120*, 12626.

(30) Parola, A. J.; Pina, F.; Ferreira, E.; Maestri, M.; Balzani, V. *J. Am. Chem. Soc.* **1996**, *118*, 11610.

(31) Frisch, M. J.; Trucks, G. W.; Schlegel, H. B.; Gill, P. M. W.; Johnson, B. G.; Robb, M. A.; Cheeseman, J. R.; Keith, T.; Petersson, G. A.; Montgomery, J. A.; Raghavachari, K.; Al-Laham, M. A.; Zakrzewski, V. G.; Ortiz, J. V.; Foresman, J. B.; Cioslowski, J.; Stefanov, B. B.;

Nanayakkara, A.; Challacombe, M.; Peng, C. Y.; Ayala, P. Y.; Chen, W.; Wong, M. W.; Andres, J. L.; Replogle, E. S.; Gomperts, R.; Martin, R. L.; Fox, D. J.; Binkley, J. S.; Defrees, D. J.; Baker, J.; Stewart, J. P.; Head-Gordon, M.; Gonzalez, C.; Pople, J. A. *Gaussian 94*, revision D.1; Gaussian, Inc.: Pittsburgh, PA, 1995.

(32) Becke, A. D. *J. Chem. Phys.* **1993**, *98*, 5648.

(33) (a) Ditchfield, R.; Hehre, W. J.; Pople, J. A. *J. Chem. Phys.* **1971**, *54*, 724. (b) Hehre, W. J.; Ditchfield, R.; Pople, J. A. *J. Chem. Phys.* **1972**, *56*, 2257. (c) Frisch, M. J.; Pople, J. A.; Binkley, J. S. *J. Chem. Phys.* **1984**, *80*, 3265.

(34) Brink, M.; Jonson, H.; Ottosson, C. *J. Phys. Chem. A.* **1998**, *102*, 6513.

(35) Cerius v3.0, Molecular Simulation Inc., San Diego, **1997**.

(36) (a) Reed, A. E.; Weinstock, R.; Weinhold, F. *J. Chem. Phys.* **1985**, *83*, 735. (b) Reed, A. E.; Curtiss, L. A.; Weinhold, F. *Chem. Rev.* **1988**, *88*, 899.

(37) The chemical shift of the amide proton of **1** appears at 9.42 ppm (CD_2Cl_2, 25 °C). The relatively low field value of this proton can be attributed to a presence of a weak side-on intramolecular hydrogen bond between this proton and the azomethine nitrogen.

(38) (a) Hidetoshi, K., et al. Presented at the International Congress of Photographic Science Meeting, Belgium, **1998**. (b) Saito, N.; Ichijima, S. Presented at the International Symposium on Silver Halide Imaging, 1997. These references are for work from the research laboratories of Fuji Photo Film Co. Kanagawa, Japan, and include compounds of type **1**, with the keto-substituent = *tert*-butyl, phenyl, and cyclopropyl. Other unpublished structures exhibiting the same conformation of S_{0a} have been solved at Kodak.

(39) (a) Henke, S. L.; Hadad, C. M.; Morgan, K. M.; Wiberg, K. B.; Wasserman, H. H. *J. Org. Chem.* **1993**, *58*, 2830. (b) Arrieta, A. F.; Haglund, K. A.; Mostad, A. *Acta Chem. Scand.* **1995**, *49*, 918. (c) Beddoes, R. L.; Cannon, J. R.; Heller, M.; Mills, O. S.; Patrick, V. A.; Rubin, M. B.; White, A. H. *Aust. J. Chem.* **1982**, *35*, 543.

(40) Brown, G. H.; Figueras, J.; Gledhill, R. J.; Kibler, C. J.; McCrossen, F. C.; Parmerter, S. M.; Vittum, P. W.; Weissberger, A. *J. Am. Chem. Soc.* **1957**, *79*, 2919.

(41) (a) Turro, N. J. *Modern Molecular Photochemistry*; Benjamin/Cummings Publishing Co.: Menlo Park, CA, 1978. (b) Michl, J.; Bonacic-Koutecky, V. *Electronic Aspects of Photochemistry*; John Wiley and Sons: New York, 1990. (c) Klessinger, M.; Michl, J. *Excited States and Photochemistry of Organic Molecules*; VCH Publishers: New York, 1995. (d) Grabowski, Z. R.; Dobkowski, J. *Pure Appl. Chem.* **1983**, *55*, 245.

(42) Brennan, C. M.; Caldwell, R. A.; Elbert, J. E.; Unett, D. J. *J. Am. Chem. Soc.* **1994**, *116*, 3460.

(43) In warm cyclohexane the two visible peaks of **3** in the absorption band appear to have nearly similar areas. Large overlap between these peaks two precludes accurate estimation their areas and λ_{max}.

(44) The two anilide protons of **3** in CD_2Cl_2 at 30 °C appear as sharp peaks at 8.47 and 9.37 ppm in the NMR spectrum. Upon cooling, the peak at 8.47 ppm (peak width = 6.6 Hz) is gradually shifted to lower field values, and is slightly broadened, reflecting presence of two rapidly exchanging species in solution having very different environments around this amide proton. At −70°, the chemical shift of this peak is 9.56 ppm, and the peak width is 18.7 Hz. These environments are consistent with presence or absence of a strong intramolecular H-bond involving this proton. The value of the peak at 9.37 ppm is similar to the chemical shift of the anilide proton of **1** (9.42 ppm), and may therefore be attributed to a proton having a side-on intramolecual H-bond with the azomethine nitogen. The chemical shift of this proton does not change upon cooling. All these results are consistent with the proposition that the two exchanging species differ only in the rotation of one of the anilide groups. We thank Andrew Hoteling for doing the NMR measurements.

(45) Kavarnos, G. J. *Fundamentals of Photoinduced Electron Transfer*; VCH Publishers: New York, 1993.